

DEVELOPMENT OF LINEAR ACTUATOR FOR SMART FACTORY

Chung Tan Lam*, Truong Trong Toai†

*Posts and Telecommunications Institute of Technology

† 3C Machinery Co., Ltd

Abstract: In this paper, a point-to-point positioning controller based on Active Disturbance Rejection Control (ADRC) is applied to a linear motion actuator using lead ball screw. In the design, the Extended State Observer (ESO) is adopted to the controller structure, and the ADRC is designed which consists of the ESO and the nonlinear PD controller to estimate and compensate the disturbances. The basic feature of the controller is that the control can apply to the plant without explicit mathematical modeling. The simulation results have been done to illustrate the stability and performance robustness of the control law.

Keywords: linear actuator, smart factory.

I. INTRODUCTION

The course of modernizing the production method drives the advance of motion control technology. The proportional-integral-derivative (PID) control has shown the effectiveness with the underlining principle in linear control, so that it remains as the choice in over 90% of industrial applications; some other control methods - such as feedback linearization, Lyapunov method, backstepping, adaptive control, sliding mode control have been a more challenging in nonlinear control.

The development and application of motion control to mechanical system can be found in almost every field of industry world wide. In motion control, the challenge is that the control system is robust in terms of insensitivity to large parameter variations of the system and the capability in disturbance rejection.

In recent years, disturbance observer techniques are often used in a motion control of a mechanical system. And there have been several researches on this technique. A high gain observer was first introduced by Khalil and Esfandiary [1] for the design of output feedback controllers due to its ability to robustly estimate the unmeasured states while asymptotically attenuating disturbances which has been used in solving many nonlinear system problems. Another proposed observer design is based on the sliding mode principle introduced by Slotine [2] and Utkin [3]. The sliding mode design method enhances robustness over a range of system uncertainties and disturbances. R. Sreedhar, et.al., used

sliding mode control for robust fault detection in nonlinear system [4]. Yao and Tomizuka proposed a new approach adaptive robust control (ARC) [5] for high performance robust control of uncertain nonlinear systems in the presence of both parametric uncertainties and uncertain nonlinearities. The approach effectively combines the design techniques of adaptive control (AC) and those of deterministic robust control (DRC) - such as sliding mode control (SMC) and improves performance by preserving the advantages of both. What's more, a class of nonlinear extended state observer was proposed by J. Han [6] in 1995 as a unique observer design. It is rather independent of mathematical model of the plants, thus achieving inherent robustness. It was tested and verified in key industrial control problem [7, 8].

In this paper, a point-to-point positioning controller based on Active Disturbance-Rejection Control was applied to a linear motion actuator using lead ball screw. In this approach, the disturbances are estimated using and extended state observer (ESO) and compensated during each sampling period. This method was developed by J. Han [5] and shown that it is a promising new technology. The ADRC consists of the ESO and a nonlinear PD controller, and it is designed without an explicit mathematical model of the plant. Once it is set up, no tuning is needed for start up, or to compensate for changes in the system dynamics and disturbances. This method is robust and has disturbance rejection capabilities, so it is suitable for this application totally. The simulations have been done to shown the effectiveness of the controller.

II. SYSTEM DESCRIPTION

A. Linear Actuator

Lead screws are widely used in converting rotary motion into linear motion. The ball screw uses precision ground ball bearings in a groove. The screw and the nut do not touch each other. Ball bearings in the grooves between the screw and the nut recirculate as the screw (or nut) rotates. When the balls reach trailing end of the nut, they are guided by a return tube back to the leading end of the nut and continue to recirculate [13]. Reduced backlash and friction makes ball screws very popular in motion control applications.

For a mechanical hardware, the rotation of a BLDC motor is converted into a translational motion by a high precision lead ball screw. A slide

Contact author: Lam Chung Tan

Email: lamct@ptithcm.edu.vn

Manuscript received: 25/5/2022, revised: 24/8/2022, accepted: 22/9/2022.

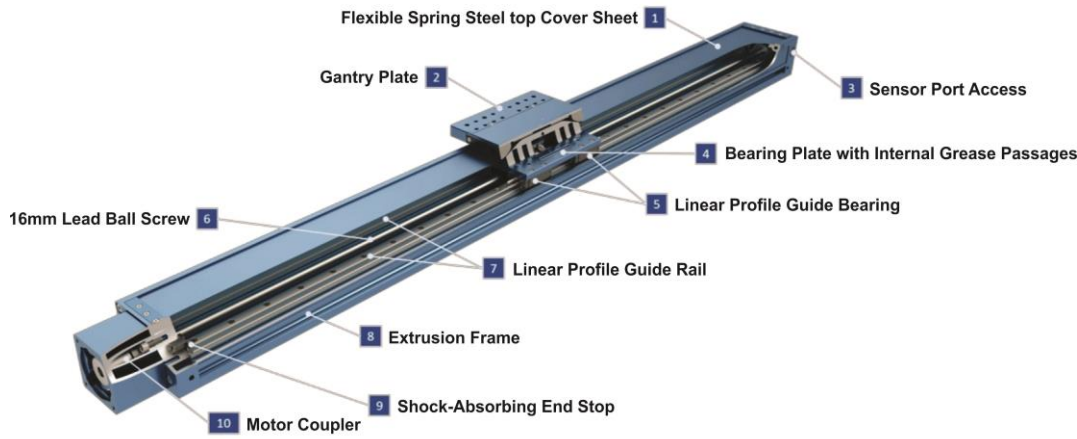


Figure 1. Linear actuator composition B. Control System

table attached to the ball-nut carries the load at high velocities. The composition of a linear actuator is shown in Fig. 1 with the following explanation:

- [1]. A thin **spring-steel cover** seals off the top of the enclosed ball screw actuator, keeping contaminants out and eliminating pinch points. The cover is held down by magnetic strips mounted in the extrusion body.
- [2]. The **gantry plate** offers 32 holes for mounting components, as well as an easy-access grease point that lubricates all moving components in the actuator at the same time.
- [3]. **Sensor port access** for home and end of travel detection. The ports come with pre-installed plugs.
- [4]. The **bearing plate** connects four linear profile guide bearings together and attaches them to the gantry plate. It also features grease passages that evenly distribute lubricant to all components.
- [5]. **Linear profile guide bearings** provide excellent strength and rigidity.
- [6]. The **lead ball screw** provides extremely accurate, rigid, and high-force actuation for extreme applications.
- [7]. **Linear profile guide rails** locate the linear ball bearings. Two rails are installed in each actuator for maximum rigidity in all directions.
- [8]. A specially designed **extrusion profile** provides the outer structure, as well as mounting points for other components. The frame is 135 mm wide and 90 mm tall.
- [9]. **Shock absorbing end-stops** are pre-installed on the actuator; there is no need for external bump stops.
- [10]. The **motor** is connected to a zero-backlash coupling for efficient and accurate power transmission.

For the control hardware, the function block of the linear actuator control hardware is shown in Fig. 2. The reference design of motor driver is referred to [14] with several modifiers for linear actuator. Main control board includes a motor driver based on STM32F405RGT6 at 120Mhz MCU and a DRV8323 bridge driver which drives 6 N-channel IRFS7530TRL7PP MOSFETs. The EtherCAT Slave Control interface is implemented for controlling from EtherCAT Master in realtime operations. This board is responsible for running the low-level motor commutation and PID controllers for separate position, velocity, and torque control at 10 kHz [14]. The QEI interface is an encoder reader which senses position of the motor that needs for the controller design.

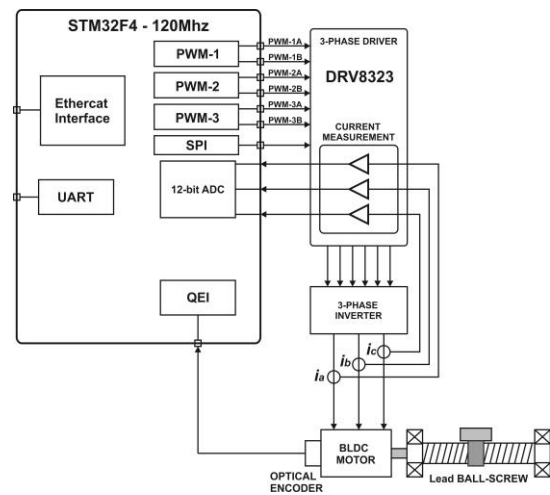


Figure 2. Function block of the linear actuator

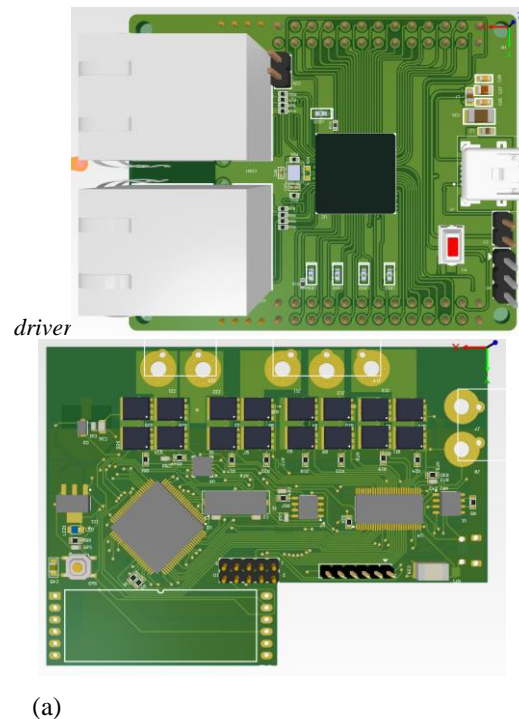


Figure 3. (a) EtherCAT communications board (b) BLDC motor driver with motion controller.

C. Motion Profile

The general equation of motion is as follow [14]:

$$s = s_0 + v_0(t - t_0) + \frac{1}{2}a(t - t_0)^2 \quad (1)$$

where t_0 is the initial time, v_0 is the initial velocity, and s_0 is the initial position. The acceleration “a” is constant.

In motion, there are two commonly used motion profiles: Trapezoidal velocity profile and S-curve velocity profile. The trapezoidal velocity profile is popular due to its simplicity. The S-curve velocity profile leads to smoother motion. To move an axis of machine, usually the following desired motion parameters are known:

- Move velocity: v_m
- Acceleration: a
- Distance to be traveled by the axis: L

The desired motion profile can be programmed into the motion controller by first specifying the move velocity and move time for the motion. Then, the program commands the axis to move through distance s .

To calculate the move time t_m , we can apply the geometric rules to Figure 4 starting with the slope of the velocity curve $a = v_m / t_a$:

$$t_a = t_d = \frac{v_m}{a} \quad (2)$$

The acceleration and deceleration times do not have to be equal but this is often the case. The total motion time is as follows:

$$t_{total} = t_a + t_m + t_d \quad (3)$$

The move time can then be found as

$$t_m = \frac{L}{v_m} - t_a \quad (4)$$

The motion controller can compute the axis position at any instant. Since the motion consists of three phases, this equation must be computed using the correct boundary values (t_0, v_0, s_0) in each segment of the motion. The move time must first be calculated using Eqs (2) and (4).

For $0 \leq t \leq t_a$: $t_0 = 0, v_0 = 0, s_0 = 0$

$$s(t) = \frac{1}{2}at^2 \quad (5)$$

For $t_a < t \leq (t_a + t_m)$:

$t_0 = t_a, v_0 = v_m, s_0 = s(t_a), a = 0$

$$s(t) = s(t_a) + v_m(t - t_a) \quad (6)$$

where $s(t_a)$ is the position from Equation (5) at t_a .

For $(t_a + t_m) < t \leq t_{total}$:

$t_0 = t_a + t_m, v_0 = v_m, s_0 = s(t_a + t_m)$

$$s(t) = s(t_a + t_m) + v_m[t - (t_a + t_m)] - \frac{1}{2}a[t - (t_a + t_m)]^2 \quad (7)$$

where $s(t_a + t_m)$ is the position from Eq. (6) at $t = (t_a + t_m)$. Note that the acceleration is negative.

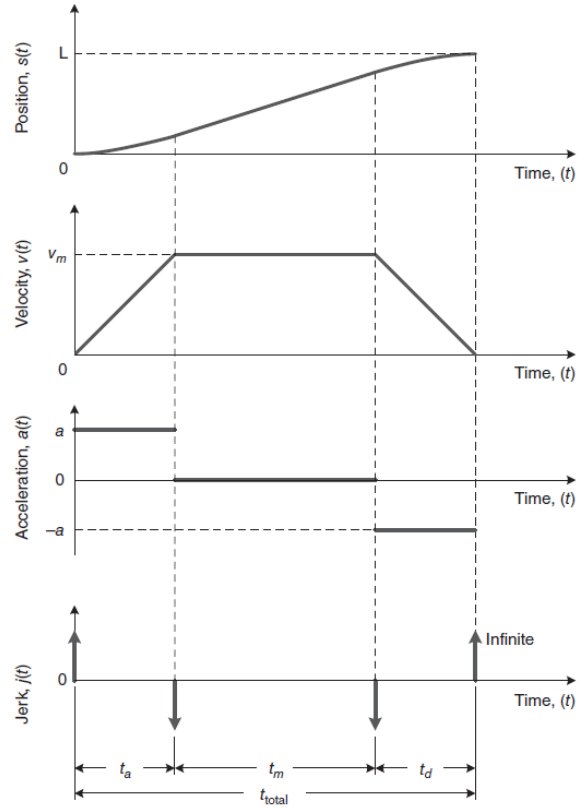


Figure 4. Trapezoidal velocity profile with position, acceleration, and jerk profiles to move an axis from 0 to position L .

III. ACTIVE DISTURBANCE REJECTION CONTROLLER

In positioning applications, the major obstacles for high performance are caused by the uncertainties due to friction and mechanical flexibility. First, it is clear that an accurate friction model is usually difficult to obtain because of its characteristics of time-variation during changing environmental parameters; furthermore, the accuracy of the friction model and updating speed are highly questionable because of the limitation on sampling rates. The second problem is the uncertain dynamics owing to the inherent flexibility of the machine structure, that is, the finite stiffness of the long ball screws as well as of other compliant links. This flexibility is a destabilizing factor in the feedback control loop, resulting in substantial limitation of the control bandwidth.

The motion equation of applications using motor as the power source can be expressed in the following form [8]:

$$\ddot{y} = f(t, y, \dot{y}, w) + bu \quad (8)$$

where y is position; u is the motor current; b is the torque constant; and w represents the external disturbance such as vibrations and the torque disturbances. The friction, the effect of inertia and various other nonlinearities in the motion system are all represented by the time-varying function $f(\cdot)$.

The state space form of Eq. (8) is as follows:

$$\begin{cases} \dot{x}_1 = x_2 \\ \dot{x}_2 = f(t, x_1, x_2, w) + bu \\ y = x_1 \end{cases} \quad (9)$$

In this paper, the following concept is applied: in order to control the system Eq. (9), it is not necessarily to analyze the expression of $f(\cdot)$ or its approximation as long as it can be estimated closely in real time and make adjustments at each sampling time in the controller. A simplistic approach is

$$\hat{f}(t, x_1, x_2, w) = bu - \dot{x}_2 \quad (10)$$

which requires the measurement or estimation of the acceleration, \dot{x}_2 .

The Extended State Observer (ESO) [8] is a unique nonlinear observer designed to estimate $f(\cdot)$. The $f(\cdot)$ is augmented as a state for the system as follows:

$$\begin{cases} \dot{x}_1 = x_2 \\ \dot{x}_2 = x_3 + bu, \quad x_3(t) \triangleq f(t, x_1, x_2, w) \\ \dot{x}_3 = h(t) \\ y = x_1 \end{cases} \quad (11)$$

where $h(t)$ is the derivative of $f(\cdot)$ and is unknown.

The following nonlinear observer is denoted as the *Extended State Observer* (ESO) and is used to estimate x and therefore $f(\cdot)$:

$$\begin{cases} \dot{z}_1 = z_2 - \beta_{01}g_1(z_1 - y(t)) \\ \dot{z}_2 = z_3 - \beta_{02}g_2(z_1 - y(t)) + b_0u \\ \dot{z}_3 = -\beta_{03}g_3(z_1 - y(t)) \end{cases} \quad (12)$$

where z_1, z_2 and z_3 are the estimates of x_1, x_2 and $x_3 = f(\cdot) = f(t, x_1, x_2, w)$, respectively. β_{01}, β_{02} and β_{03} are observer gain, b_0 represents the nominal value of the torque constant and $g_1(\cdot), g_2(\cdot)$ and $g_3(\cdot)$ are appropriate linear or nonlinear functions. They are chosen as follows [8]:

$$g_i(\varepsilon) = fal(\varepsilon, \alpha, \delta) = \begin{cases} |\varepsilon|^\alpha \text{sign}(\varepsilon), & |\varepsilon| > \delta \\ \frac{\varepsilon}{\delta^{1-\alpha}}, & \text{otherwise} \end{cases} \quad (13)$$

As α_i is chosen between 0 and 1, g_i yields high gain when error is small δ is a small number used to limit the gain in the neighborhood of origin; in other words, the function $fal(\varepsilon, \alpha, \delta)$ introduces a small linear region in the gain function. The purpose of this gain function is to prevent excessive gain when error is small, which is known to cause high frequency chattering. This technique is widely used in industrial applications.

There are several following remarks [7]:

- (1) The nonlinear function in Eq. (13) is used to make the observer more efficient. It was selected

heuristically based on experimental results. Intuitively, it is a nonlinear gain function where small errors correspond to higher gains. This technique is used widely in industrial applications

- (2) If $g_i(e) = e$ are chosen (linear function), the ESO take the form of classical Luenberger observer. Also, if $g_i(e) = e + k_i \text{sign}(e)$, the ESO becomes sliding mode observer.
- (3) The observer Eq. (12) reflects the knowledge of the system, that is, if the plant is given more information, such as friction, the system is more effective.
- (4) There is a linear segment in Eq. (13) in the neighborhood of the origin. It was discovered that the nonlinear function in Eq. (13) makes the observer converge faster than the linear counterpart, and the linear segment in Eq. (13) makes the output of the observer smoother.
- (5) The proper selections of the gains and functions in Eq. (12) are critical to the success of the observer. One approach is to design the linear observer first and then gradually increase the nonlinearity to improve the performance. It was discovered that once the ESO is properly setup, the performance of the observer is quite insensitive to the plant variations and disturbances.

The architecture of ADRC is shown in Fig. 5. It consists of three components: Profile Generator, Extended State Observer (ESO) and Nonlinear PD. The control law is defined as

$$u(t) = u_0(t) - z_3(t) / b_0 \quad (14)$$

which reduces the plant to the double integrator, which is, in turn, controlled by the nonlinear PD controller:

$$u_0(t) = k_p f_1(e_1) + k_D f_2(e_2) \quad (15)$$

where $e_1 = v_1 - z_1$ and $e_2 = v_2 - z_2$ are the position and velocity error, respectively; k_p and k_D are the gains of the PD controller; and $f_1(\cdot)$ and $f_2(\cdot)$ are appropriate nonlinear functions, such as the one in Eq. (13).

The Profile Generator generates the desired output trajectory, $v_1(t)$ and $v_2(t) = \dot{v}_1(t)$. Then, they are compared to the filtered output $z_1(t)$ and $z_2(t) = \dot{z}_1(t)$. It can be seen that the differentiation of the error is obtained without directly taking the differentiation of the setpoint or the output; this behavior make the system much less sensitive to noises in the output and discontinuities in the setpoint $r(t)$.

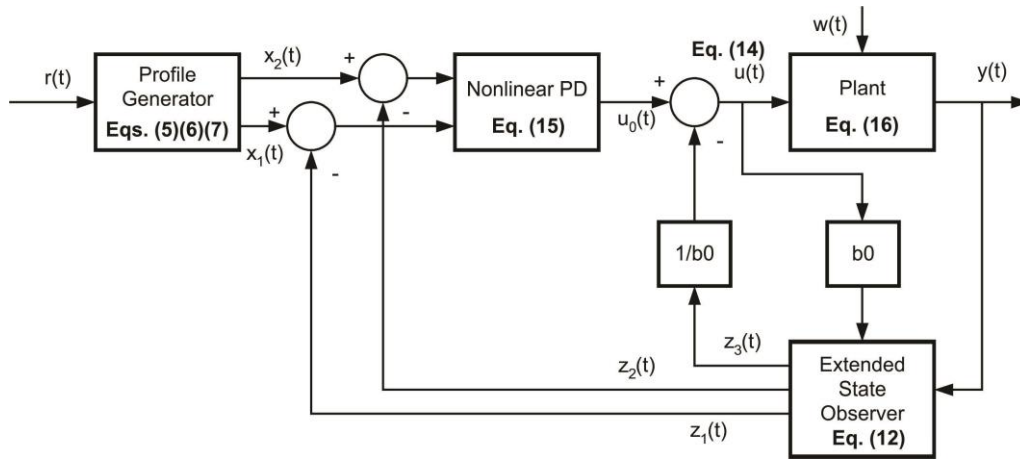


Figure 5. Active Disturbance Rejection controller scheme

Simulation Results

To verify the effectiveness of the proposed controller, simulations have been done with controller Eq. (14) with the trapezoidal profile produced by profile generator as in Figs. 6 and 7. The ESO enables the controller to actively compensate for the changes in the dynamics (inertia) or the disturbances (constant torque disturbance). Mathematically, in the presence of the torque disturbances, $T_d(t)$, the dynamic equation of the plant can be written as

$$\ddot{y} = (-1.4\dot{y} + 23.2\tau_d - 7.51u) + 30.71u \quad (16)$$

or $\ddot{y} = (-1.41\dot{y} + 23.2T_d) + 23.2u$

The function to be estimated is

$$f(.) = a(t) = -1.41\dot{y} + 23.2T_d - 7.51u \quad (17)$$

The position estimation value z_1 in comparison with the state value x_1 and the reference value v_1 is shown in Fig. 8; the velocity estimation z_2 , state value x_2 and the reference value v_2 is shown in Fig. 9; and the unknown system dynamic estimation in Fig. 10, respectively. In Figs. (11)-(14), it is shown that all three outputs of the ESO track their targets as desired. The control input is shown in Fig. 15.

The control system was setup but the experimental data have not been achieved at this time of writing. The experimental data will be included in the future work.

To see the effectiveness of the ESO, the plot of $z_3(t)$ and its target $a(t)$ is shown in Fig. 7, and it is shown that $z_3(t)$ tracks $a(t)$ very closely.

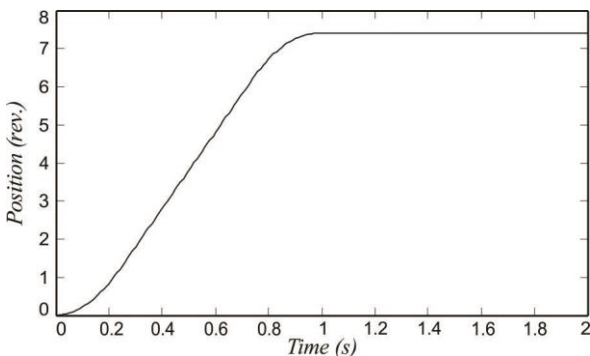


Figure 6. Position (Trapezoid) profile

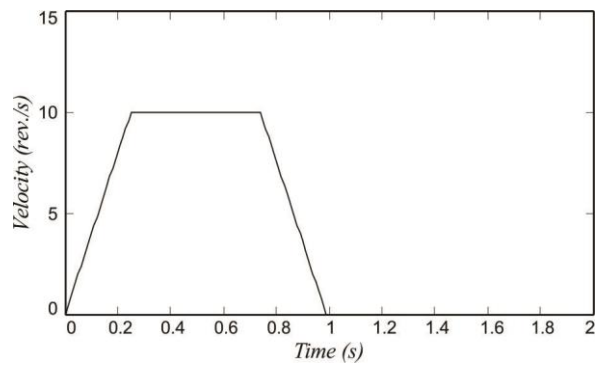


Figure 7. Velocity (Trapezoid) profile

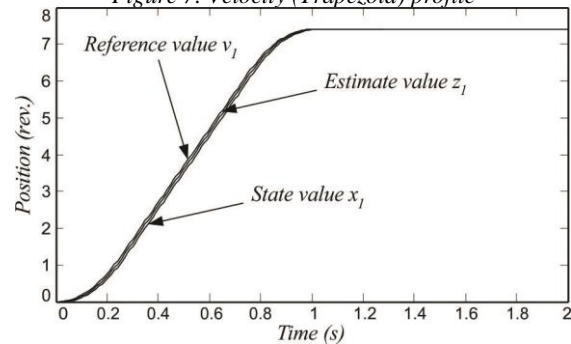


Figure 8. Position estimation

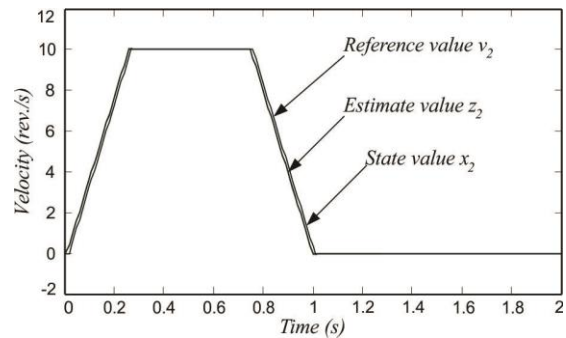


Figure 9. Velocity estimation

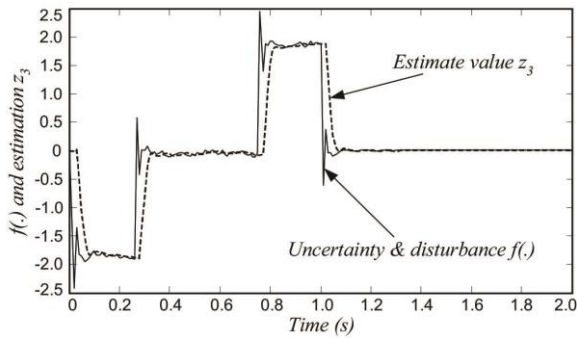


Fig. 10 The estimation of disturbances $f(.)$

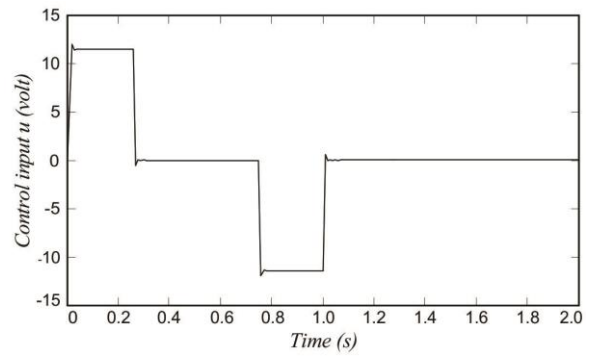


Figure 15. Control input u

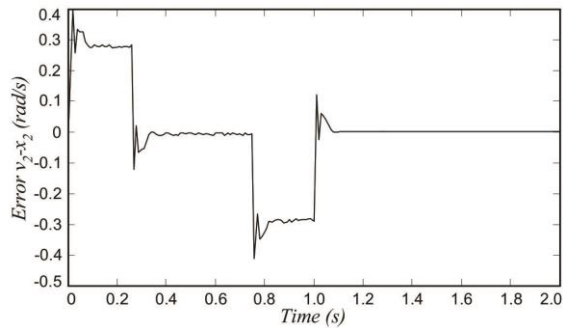


Fig. 11 Velocity reference-estimation error (v_2-x_2)

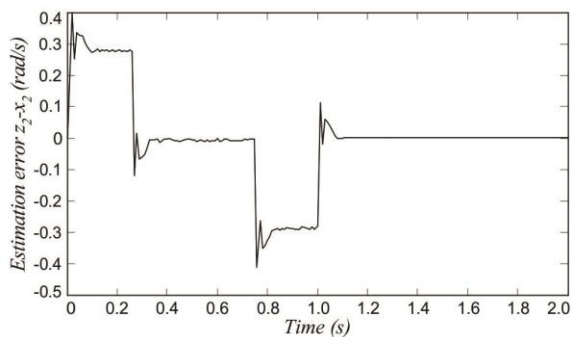


Fig. 12 Velocity state-estimation error (z_2-x_2)

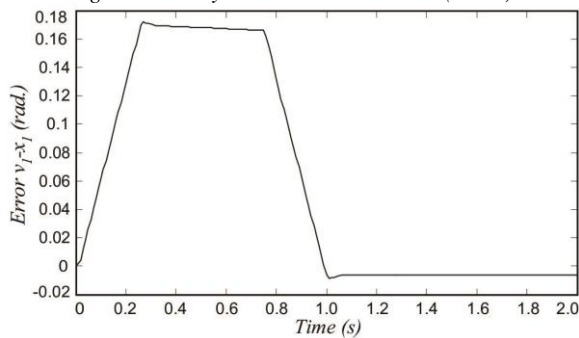


Fig. 13 Position reference-estimation error (v_1-x_1)

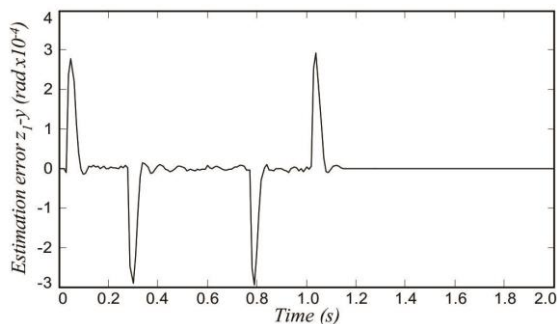


Fig. 14 Error of output and estimation (z_1-y)

For the application, the smart linear actuator is ready to cooperate with cobot to become mobile cobot in the fields of Industrial 4.0. This configuration has been widely used to extend tasks for cobot in the automation factory. The illustration of this field is shown in Fig. 16.

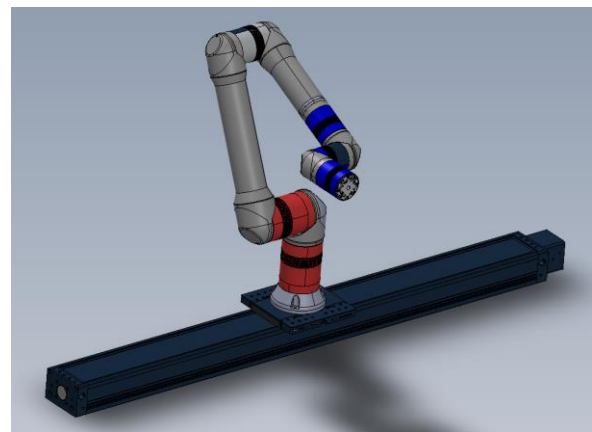


Figure 16. The application of smart linear actuator - mobile cobot

V. CONCLUSIONS

A motion control concept has been considered to the linear motion actuator using lead ball screw. The scheme of Active Disturbance Rejection control is applied to the actuator. The Extended State Observer is adopted to the controller structure which consists of the ESO and the nonlinear PD controller to estimate and compensate the disturbances. This technology gives good performance for industrial applications for its intuitive and inherently robust; moreover, it does not require an explicit model of the plant. So this approach perhaps gives control practitioners another alternative. The initial result also provides researchers with a new direction in developing truly robust control design methodology. It is needed for it to be verified over the practical field.

ACKNOWLEDGMENT

This research is supported by Vingroup Innovation Foundation (VINIF) in project code VINIF.2020.NCUD.DA059

REFERENCES

- [1] F. Esfandiari and H.K Khalil "Output feedback stabilization of fully linearizable system," International Journal of Control, 56. pp. 1007-1037, 1992.
- [2] J.J.E Slotine., J.K Hedrick, and E.A. Misawa "On Sliding

AUTHORS

- Observers for nonlinear system,” *Journal of Dynamics Systems, Measurement and Control*,” Vol, 109, pp. 245-252, 1987.
- [3] V.I. Utkin, “Sliding-modes in Control Optimization,” Springer-Verlag, 1992.
- [4] R. Sreedhar, B. Fernandez, and J.Y. Masawa, “Robust Fault Detection in Nonlinear System Using Sliding Mode Observer,” *Proceedings of IEEE Conference on Control and Applications*, Vancouver, BC, 1993.
- [5] B. Yao and M. Tomizuka “Adaptive And Robust Control of Robot Manipulators: Theory and Comparative Experiment,” *Proceedings of IEEE Conference on Decision and Control*, pp. 1290-1295, 1994.
- [6] Y. Huang and J. Han. "Analysis and Design for Nonlinear continuous Extended State Observer," *Chinese Science Bulletin*, 45, pp. 1373-1379, 2000.
- [7] Y. Hou, Z. Gao, F. Jiang and B.T. Boulter, "Active Disturbance Rejection Control For Web Tension Regulation," *Proceedings the 40th IEEE Conference on Decision and Control*, Orlando, Florida USA, December 2001, pp. 4974-4949.
- [8] Z. Gao, S. Hu and F. Jiang, “A Novel Motion Control Design Approach Based On Active Disturbance Rejection,” *Proceedings of the 40th IEEE Conference on Decision and Control*, Orlando, Florida USA, December 2001, pp. 4877-4882.
- [9] Z. Gao, Y. Huang and J. Han, “An Alternative Paradigm for Control System Design,” *Proceedings of the 40th IEEE Conference on Decision and Control*, Orlando, Florida USA, December 2001, pp. 4578-4585.
- [10] George Ellis, "Control System Design Guide", 2nd Edition, Academic Press, 2000.
- [11] M. Tomizuka, “Controller Structure for Robust High-Speed/High-Accuracy Digital Motion Control,” in *Notes for the tutorial session at the 1994 IEEE Conference on Robotics and Automation*, 1994.
- [12] Lee H. S. and Tomizuka M., “Robust Motion Controller Design for High Accuracy Positioning Systems,” *IEEE Trans. on Industrial Electronics*, Vol, 43, No. 1, pp. 48-55, 1996.
- [13] Hakan Gürocak (2016), *Industrial Motion Control, Motor Selection, Drives, Controller Tuning, Application*, John Wiley & Sons, Ltd..
- [14] Chung Tan Lam and Truong Trong Toai, “Development of a Collaborative Robot-VietCobot,” *Journal of Science and Technology on Information and Communications*,” Vol. 1, CS.01, pp. 30-42, 2021.
- [15] Chung Tan Lam and Truong Trong Toai, “Neural Network Control of VietCobot,” *Journal of Science and Technology on Information and Communications*,” Vol. 3, CS.01, pp. 21-31, 2021.

NGHIÊN CỨU PHÁT TRIỂN CƠ CẤU CHẤP HÀNH TUYẾN TÍNH CHO NHÀ MÁY THÔNG MINH

Tóm tắt: Bài báo này trình bày ứng dụng một bộ điều khiển vị trí dựa trên Active Disturbance Rejection Control (ADRC) vào một cơ cấu chấp hành tuyến tính loại trục vít me đai ốc bi. Trong thiết kế, Extended State Observer (ESO) được đưa vào cấu trúc bộ điều khiển và ADRC được thiết kế bao gồm ESO và bộ điều khiển PD phi tuyến để ước lượng và bù trừ nhiễu ngoài. Đặc tính cơ bản của bộ điều khiển này là điều khiển có thể ứng dụng cho loại hệ thống không có mô hình toán rõ ràng. Mô phỏng được thực hiện để minh họa cho tính ổn định và bền vững của luật điều khiển dưới sự tác động của tải và nhiễu khác nhau.



Chung Tan Lam, He received Master of Mechanical Design from Department of Mechanical Engineering, Pukyong National University, Pusan, Korea in 2002. He received Ph.D of Mechatronics from Pukyong National University in 2006. Currently, he is Head of Automatic Control Division, Electronics Department 2, PTIT-HCM. His research interests are Factory Automation, Modelling and Control of Robotics, Embedded systems, Realtime Communications in Robotics, Cobots and Smart Actuators, Mobile Robots.



Truong Trong Toai, He is Vice Director of 3C Machinery Co. Ltd., established in 2014. The company is one of the leading R/D in robotics fields in HoChiMinh City, Vietnam. The company got the Price “Vietnam's Rice Bowl Starup Awards” in 2017. His research interests are Solutions of Industrial Robotics for SMEs, Smart Devices, Modernizing Industrial Production Process, Collaborative robots and Smart Actuators